

Kinematics and optimization of a 2-DOF parallel manipulator with a passive constraining leg and linear actuators[†]Ji-Hoon Lee¹, Yun-Joo Nam¹ and Myeong-Kwan Park^{2,*}¹Department of Mechanical Engineering, Pusan National University, Busan, 609-735, Korea²Research Institute of Mechanical Technology, Pusan National University, Busan, 609-735, Korea

(Manuscript Received May 1, 2009; Revised September 30, 2009; Accepted October 12, 2009)

Abstract

This paper presents a two degree-of-freedom (DOF) planar parallel manipulator with two linear actuators, whose degree of freedom is dependent on a passive constraining leg connecting the base and the platform. The kinematics of the presented manipulator is first studied: the inverse and forward kinematics problems are solved in the closed form, the practical workspace is described symbolically, the Jacobian matrix is derived, and several singular conditions are discussed. Then, in order to determine the geometric parameters and the operating range of the actuators, the optimization of the mechanism is performed considering its dexterity and stiffness.

Keywords: Kinematics; Limited-DOF mechanism; Optimal design; Parallel manipulator; Passive constraining leg

1. Introduction

The manipulator introduced in this paper is a 2-DOF planar parallel manipulator which consists of two identically actuated legs with three degree-of-freedom and one passive constraining leg with two degree-of-freedom, connecting the platform and the base. The degree-of-freedom of the manipulator is dependent on the passive leg's degree of freedom, and therefore the moving platform has two degrees of freedom: one degree of translational freedom and one degree of rotational freedom, with respect to the base. In what follows, the kinematics of the presented manipulator is analyzed: the inverse and forward kinematics problems are solved in the closed form, the practical workspace is described symbolically, the Jacobian matrix is derived, and several singular conditions are discussed. Then, in order to determine the geometric parameters and the operating range of the actuators, the optimization of the mechanism is performed in terms of dexterity, stiffness and workspace. The results of this paper can be of great help in the design, application and control of such devices.

2. Description of the manipulator

The 2-DOF parallel manipulator studied in this (Fig. 1) consists of a moving platform that is connected to a fixed base by

three legs. Two of the three legs, called the actuated leg, have kinematically identical topology. The i th actuated leg l_i ($i = 1, 2$) connects point B_i on the base to point b_i on the moving platform by a passive revolute joint followed by an active prismatic joint and another passive revolute joint. The third leg l_c is a passive constraining leg and has architecture different from the other legs, one end of which is fixed perpendicularly at the center C of the moving platform and the other is jointed at the center O of the base by a passive revolute joint followed

by a passive prismatic joint. Here, the geometric parameters of the mechanism are $r = |Cb_i|$ and $R = |OB_i|$, which designate the sizes of the moving platform and the base, respectively.

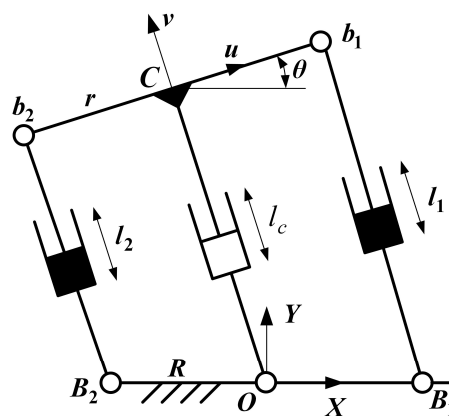


Fig. 1. 2-DOF parallel manipulator with a passive constraining leg.

[†] This paper was presented at the ICMDT 2009, Jeju, Korea, June 2009. This paper was recommended for publication in revised form by Guest Editors Sung-Lim Ko, Keiichi Watanuki.

*Corresponding author. Tel.: +82 51 510 2464, Fax.: +82 51 510 0685

E-mail address: mkpark1@pusan.ac.kr

© KSME & Springer 2010

3. Position kinematics

Considering that the passive constraining leg should be fixed perpendicularly to the moving platform, the relationship between the independent and dependent variables is given by

$$x_c \cos \theta + y_c \sin \theta = 0 \quad (1)$$

3.1 Inverse kinematics

The inverse kinematics is to find a set of input joint variables for a given position and orientation of the moving platform with respect to the base. For the presented manipulator, the output variables (x_c, y_c) are given, and the input joint variables (l_1, l_2) are to be found.

Referring to Fig. 1, the closed-loop equations for each actuated leg are written as

$$l_1 = \pm \sqrt{(x_c + r \cos \theta - R)^2 + (y_c + r \sin \theta)^2} \quad (2)$$

$$l_2 = \pm \sqrt{(x_c - r \cos \theta + R)^2 + (y_c - r \sin \theta)^2} \quad (3)$$

Only positive leg lengths should be taken into consideration for real applications, since negative solutions could only be obtained by reassembling the mechanism.

3.2 Forward kinematics

The forward kinematics is to find the position and orientation of the moving platform corresponding to a given set of input joint variables. For the given mechanism, the inputs (l_1, l_2) are known, and the pose of the moving platform (x_c, y_c) is to be found.

Referring to (1) and the architecture of the manipulator yields

$$\begin{cases} x_c = -l_c \sin \theta \\ y_c = l_c \cos \theta \end{cases} \quad (4)$$

where $l_c = (x_c^2 + y_c^2)^{1/2}$ is the length of the passive constraining leg. Substituting (4) into (2) and (3) and rearranging leads to

$$l_1^2 - l_2^2 = 4l_c R \sin \theta \quad (5)$$

$$l_1^2 + l_2^2 = 2l_c^2 + 2r^2 + 2R^2 - 4Rr \cos \theta \quad (6)$$

Applying the identity $\cos^2 \theta + \sin^2 \theta = 1$ to (5) and (6), the forward kinematics expressed by a cubic polynomial in square of l_c is obtained as

$$l_c^6 + 2\alpha l_c^4 + (\alpha^2 - \beta) l_c^2 + \gamma^2 = 0 \quad (7)$$

where $\alpha = r^2 + R^2 - (l_1^2 + l_2^2)/2$, $\beta = 4R^2 r^2$, and $\gamma = r(l_1^2 - l_2^2)/2$. From (7), we can see that there are at most three forward kinematics solutions for the given input joint variables, since the passive constraining leg should become

positive lengths in real practice. With the obtained l_c and the given values l_1 and l_2 , the rotation angle θ can be uniquely determined from (5) and (6). Therefore, all possible solutions to the forward kinematics for the presented manipulator are to be three.

4. Workspace analysis

The workspace of the presented manipulator is the set of all the output variables (x_c, y_c) at which the reference point C of the moving platform can reach. In this study, in order to disregard the mechanical interferences between the links and joints, especially between the passive leg l_c and the base joints B_1 and B_2 , the range of the rotation angle of the moving platform is restricted to $\theta = \arctan(-x_c/y_c) \in (-\pi/2, \pi/2)$. In addition, the range of motion of the actuators is given by $l_1, l_2 \in [l_{\min}, l_{\max}]$.

Fig. 2 shows the geometric algorithm to obtain the boundaries of the workspace for the manipulator studied in this paper.

If inputs l_1 and l_2 are specified, (2) and (3) represent two circles in the frame $O_{-}xy$, each of which has its radius of l_i ($i=1, 2$) and its center at (x_i, y_i) . Considering that these centers are given as the function of the dependent variable θ yields the following relationships

$$(x_1 - R)^2 + y_1^2 = r^2 \quad (8)$$

$$(x_2 + R)^2 + y_2^2 = r^2 \quad (9)$$

For effectively calculating the workspace size required in the design stage of the presented manipulator, it is necessary to derive the boundaries of the workspace symbolically. The outer boundary represented by (x_{cm}, y_{cm}) is obtained whenever at least one of the actuators reaches at its maximum length l_{\max} , while the inner boundary represented by (x_{cm}, y_{cm}) at its minimum length l_{\min} . With these geometric

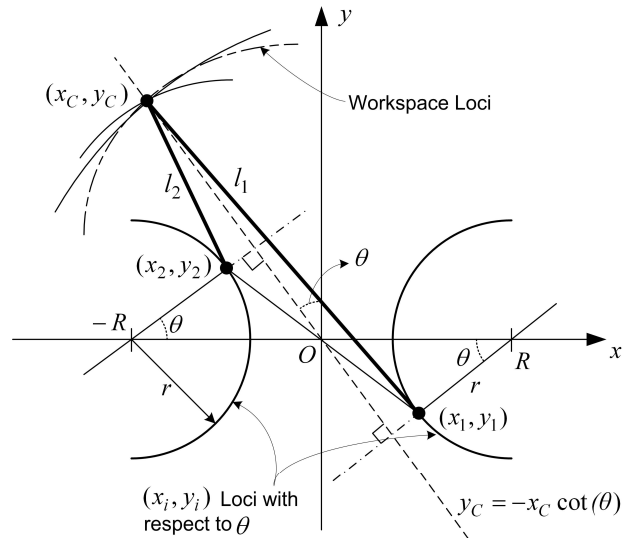


Fig. 2. Geometric algorithm for generating the boundary of workspace.

constraints, these workspace boundaries can be obtained in four cases as follows:

Case 1: $l_1 = l_{\max}$ or $l_2 = l_{\max}$ for $\theta \neq 0$

$$x_{CM} = \text{sgn}(i) \left[R - \sqrt{R^2 - \frac{R^2 + r^2 - 2rR \cos \theta - l_{\max}^2}{\sin^2 \theta}} \right] \sin^2 \theta$$

$$y_{CM} = -x_{CM} \cot \theta \quad (10)$$

Case 2: $l_1 = l_{\min}$ or $l_2 = l_{\min}$ for $\theta \neq 0$

$$y_{CM} = -x_{CM} \cot \theta \quad (11)$$

Case 3: $l_1 = l_{\max}$ and $l_2 = l_{\max}$ for $\theta = 0$

$$x_{CM} = 0, \quad y_{CM} = \sqrt{l_{\max}^2 - (R-r)^2} \quad (12)$$

Case 4: $l_1 = l_{\min}$ and $l_2 = l_{\min}$ for $\theta = 0$

$$x_{CM} = 0, \quad y_{CM} = \sqrt{l_{\min}^2 - (R-r)^2} \quad (13)$$

where the sign function $\text{sgn}(i)$ is to be “1” for $i=1$ and to be “-1” for $i=2$.

5. Jacobian analysis

5.1 Jacobian matrix

The Jacobian of the presented manipulator relates the velocities of the moving platform to the input joint rate.

$$l_1 \dot{l}_1 = (x_c + r \cos \theta - R) \dot{x}_c + (y_c + r \sin \theta) \dot{y}_c + (-x_c r \sin \theta + y_c r \sin \theta + R r \sin \theta) \dot{\theta} \quad (14)$$

$$l_2 \dot{l}_2 = (x_c - r \cos \theta + R) \dot{x}_c + (y_c - r \sin \theta) \dot{y}_c + (x_c r \sin \theta - y_c r \sin \theta + R r \sin \theta) \dot{\theta} \quad (15)$$

The angular velocity $\dot{\theta}$ should be expressed as the function of \dot{x}_c and \dot{y}_c , which can be obtained by differentiating (1) with respect to time as

$$\dot{\theta} = \frac{\dot{x}_c \cos \theta + \dot{y}_c \sin \theta}{x_c \sin \theta - y_c \cos \theta} \quad (16)$$

$x_c \sin \theta - y_c \cos \theta = 0$ implies $l_c = 0$ which cannot be achieved in practice. Substituting (16) into (14) and (15) and rearranging in vector form leads to

$$\mathbf{J}_q \dot{\mathbf{q}} = \mathbf{J}_x \dot{\mathbf{x}} \quad (17)$$

where $\dot{\mathbf{q}} = [\dot{l}_1, \dot{l}_2]^T$ and $\dot{\mathbf{x}} = [\dot{x}_c, \dot{y}_c]^T$ are defined as the input and output velocity vectors, respectively. The inverse and forward Jacobian matrices \mathbf{J}_q and $\mathbf{J}_x \in \mathcal{R}^2$ are, respectively, expressed by

$$\mathbf{J}_q = \text{diag}(l_1, l_2) \quad (18)$$

$$\mathbf{J}_x = \begin{bmatrix} x_c - R + \delta \cos \theta & y_c + \delta \sin \theta \\ x_c + R + \delta \cos \theta & y_c + \delta \sin \theta \end{bmatrix} \quad (19)$$

$$\text{where } \delta = \frac{Rr \sin \theta}{x_c \sin \theta - y_c \cos \theta}$$

Therefore, the Jacobian matrix of the presented mechanism can be written as

$$\mathbf{J} = \mathbf{J}_q^{-1} \mathbf{J}_x \quad (20)$$

The second part consisting of the paper body must be edited in double column format.

5.2 Singularity analysis

The first kind of singularity is related to matrix \mathbf{J}_q , which means that \mathbf{J}_q becomes singular but \mathbf{J}_x is invertible.

$$\det(\mathbf{J}_q) = 0 \quad ; \quad l_1 = 0 \quad \text{or} \quad l_2 = 0 \quad (21)$$

This corresponds to the configuration in which the moving platform is at or near boundary of its workspace. In such a singularity, the manipulator can resist external forces or moments without exerting any force of the actuated legs since the moving platform loses one or two degrees of freedom. However, this condition cannot be reached since the actuated leg has a positive length in practice.

The second kind of singularity occurs when \mathbf{J}_q is invertible but \mathbf{J}_x becomes singular.

$$\det(\mathbf{J}_x) = 0 \quad ; \quad R = 0 \quad \text{or} \quad x_c y_c \sin \theta - y_c^2 \cos \theta + R r \sin^2 \theta = 0 \quad (22)$$

This corresponds to the configuration in which the moving platform can move even when all the actuators are locked. In such configurations, the moving platform gains one mobility and the manipulator cannot resist an external force or moment.

The third kind of singularity, called architecture singularity [1], occurs when both \mathbf{J}_q and \mathbf{J}_x become singular simultaneously. This corresponds to the configuration in which the moving platform can locally move with all the actuators locked or in which a finite motion of the actuators cannot occur any motions of the moving platform. For the identification of such singularities, assume that one of the actuators has its length of zero. Then, in this case, the rotation angle of the moving platform θ and the length of the passive constraining leg l_c are given by

$$\theta = \arccos(r/R), \quad l_c = \sqrt{R^2 - r^2} \quad \text{for} \quad R \geq r \quad (23)$$

Substituting the above equations into the second singular condition of (22) leads to

$$l_c^2 \cos \theta = R r \sin^2 \theta \quad (24)$$

from which we can see that the architecture singularity corresponds to the first kind of singularity. In addition, the same

result is obtained even when both the actuators have zero length.

6. Optimal design

(1) Global Conditioning Index: The first performance index used in this paper as an objective function to be maximized is the global conditioning index [2, 3] defined by

$$\eta_1 = \frac{\int_w 1/\kappa dW}{\int_w dW} \quad (25)$$

where dW is differential workspace of the manipulator, and κ is the condition number of the Jacobian \mathbf{J} at a given position of the moving platform within the workspace.

(2) Global Resistivity Index: The second performance index introduced for measuring the ability of the presented manipulator to resist the externally applied forces is defined by

$$\eta_2 = \frac{\int_w \varpi dW}{\int_w dW} \quad (26)$$

where $\varpi = 1/|\det(\mathbf{J}^{-1})| = |\det(\mathbf{J})|$ is the inverse of the manipulability.

(3) Space Utilization Index: Actually, since the first two performance indices are normalized by the workspace size, they have the limitation to consider the workspace size of a manipulator. Hence, the workspace size of the presented manipulator is evaluated by the space utilization index [4] expressed as

$$\eta_3 = \frac{\int_w dW}{S} \quad (27)$$

where S is the bounding box defined as the smallest rectangle enclosing the manipulator structure and the workspace size.

It is clear that a practical optimization of the manipulator studied here would require a design index comprising multiple performance indices mentioned above. The values of the three performance indices may be distributed in different ranges. Hence, in order to make a meaningful comparison among them and to prevent simply cancellations between denominators and numerators during the combination process, each of the three indices is normalized by using their maximum and minimum values. Then, the composed design index for the workspace optimization of the presented manipulator can be defined as

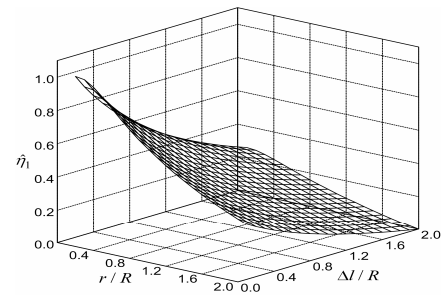
$$\eta = w_1\hat{\eta}_1 + w_2\hat{\eta}_2 + w_3\hat{\eta}_3 \quad (28)$$

The objective of the workspace optimization is to determine the set of the manipulator design parameters leading to the composed design index to be maximized. The design parameters of the presented manipulator include the operating limits of the actuated joint variables, l_{\min} and l_{\max} , and the sizes of the base and moving platforms, r and R .

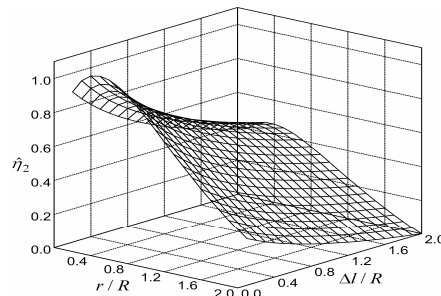
On the basis of the above analysis, assuming that $R = 1$ and the given design parameters vary in their constrained ranges, the workspace optimization problem of the presented manipulator can be defined as follows

$$\underset{r, \Delta l}{\text{Maximize}} (\eta) \quad \text{subject to } r, \Delta l \in [0, 2] \quad (29)$$

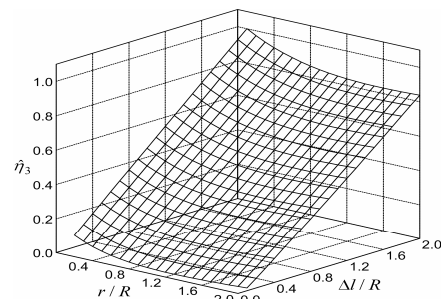
Fig. 3 shows the global isotropy index, the global resistivity index, and the space utilization index with respect to r and Δl , actually r/R and $\Delta l/R$. The global isotropy index monotonically increases as both r and Δl decrease, and its maximum value is taken at the smallest values at $r = 0$ and $\Delta l = 0$. The global resistivity index decreases as r keeps away from about $r = 0.2$ and increases slowly as Δl decreases. Moreover, the index is relatively insensitive to the variation of Δl compared to r . The space utilization index monotonically increases with the decrease of r and the increase of Δl . Also, as compared to r , the variation of Δl has more effects on this index.



(a) Normalized global conditioning index



(b) Normalized global manipulability index



(c) Normalized space utilization index

Fig. 3. Kinematic performance indices.

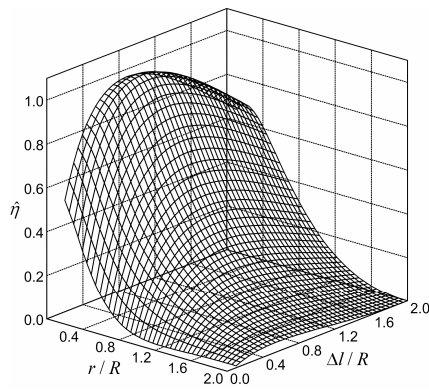


Fig. 4. Normalized composed design index.

Fig. 4 shows that the composed design index for the presented manipulator, when all of the weighting factors w_i ($i=1\sim 3$) are given by 1 such that the effects of three indices can be considered equally. Similarly to the global isotropy index, this index increases as r and Δl decrease and its minimum value is taken at the smallest values at $r=0$ and $\Delta l=0$. Moreover, the index is relatively insensitive to the variation of Δl compared to r , indicating that the workspace size of the presented manipulator can be decided rather freely.

7. Conclusion

A 2-DOF planar parallel manipulator with two linearly actuated legs and one passive constraining leg was presented. The mobility of the presented mechanism depending on one passive constraining leg is determined to be two degrees of freedom including one translational motion and one rotational motion, leading to arbitrary cylindrical motions of the moving platform.

References

- [1] Ma and J. Angeles, Architecture singularities of platform manipulator, *Proc. IEEE Int. Conf. on Robotics and Automation*, Sacramento, California, USA. (1991) 1542-1547.
- [2] F. Gao, X. Liu and W. A. Gruver, Performance evaluation of two-degree-of-freedom planar parallel robots, *Mech. Mach. Theory* 33 (6) (1998) 661-668.
- [3] Frisoli, G. M. Prisco, F. Salsedo and M. Bergamasco, A two degrees-of-freedom planar haptic interface with high kinematic isotropy, *Proc. IEEE Int. Works. on Robot and Human Interaction*, Pisa, Italy (1999) 297-302.
- [4] M. Stock and K. Miller, Optimal kinematic design of spatial parallel manipulators: application to linear delta robot, *Tran. ASME J. Mech. Des.* 125 (2) (2003) 292-301.



Ji-Hoon Lee received the B.S. and M.S. degrees from the Department of Mechanical Engineering, Pusan National University. His current research interests are hydraulic and pneumatic control, and haptic system by using smart fluids.



Myeong-Kwan Park received the M.S. and Ph.D. degrees from Tokyo Institute of Technology, Tokyo, Japan. He is currently a full professor with the Department of Mechanical Engineering and a researcher in the Research Institute of Mechanical Technology at Pusan National University.